

# The Collision Between The Milky Way And Andromeda

T. J. Cox<sup>\*</sup> and Abraham Loeb<sup>†</sup>

*Harvard-Smithsonian Center for Astrophysics, 60 Garden Street, Cambridge, MA 02138, USA*

21 February 2008

## ABSTRACT

We use an N-body/hydrodynamic simulation to forecast the future encounter between the Milky Way and the Andromeda galaxies, given current observational constraints on their relative distance, relative velocity, and masses. Allowing for a comparable amount of diffuse mass to fill the volume of the Local Group, we find that the two galaxies are likely to collide in a few billion years - within the Sun's lifetime. During the first close encounter of the two galaxies, there is a 12% chance that the Sun will be pulled from its present position and reside in the extended tidal material. After the second close encounter, there is a 30% chance that the Sun will reside in the extended tidal material, and a 2.7% chance that our Sun will be more tightly bound to Andromeda than to the Milky Way. Eventually, after the merger has completed, the Sun is likely to be scattered to the outer halo and reside at much larger radii ( $> 30$  kpc). The density profiles of the stars, gas and dark matter in the merger product resemble those of elliptical galaxies. Our Local Group model therefore provides a prototype progenitor of late-forming elliptical galaxies.

**Key words:** galaxy:evolution — galaxies:evolution — galaxies:formation — galaxies:interactions — Local Group — methods:N-body simulations.

## 1 INTRODUCTION

It is well known that the Milky Way (MW) and Andromeda (M31) are the two largest members of the Local Group of galaxies. Together with their  $\sim 40$  smaller companions, the Milky Way and Andromeda comprise our galactic neighborhood, and as such, represent the nearest laboratory, and therefore the most powerful tool, to study the formation and evolution of galactic structure.

Like most extragalactic groups, the Local Group is very likely to be decoupled from the cosmological expansion and is now a gravitationally bound collection of galaxies. This notion is supported by the observed relative motion between its two largest galaxies; namely, the Milky Way and Andromeda are moving toward each other at  $\sim 120 \text{ km s}^{-1}$  (Binney & Tremaine 1987). Unfortunately, this motion alone does not indicate whether the Local Group is bound or not. The unknown magnitude of Andromeda's transverse velocity adds uncertainty into the present day orbital parameters and therefore the past and future evolution of the Local Group.

Barring the uncertain transverse velocity of Andromeda, a considerable amount of information can be in-

ferred about the Local Group provided a plausible set of assumptions. Nearly 50 years ago Kahn & Woltjer (1959) pioneered the “timing argument,” in which the Milky Way and Andromeda are assumed to form within close proximity to each other, during the dense early stages of the Universe, before they were pulled apart by the general cosmological expansion. They have subsequently reversed their path and are approaching one another owing to their mutual gravitational attraction. According to the timing argument, the Milky Way and Andromeda have now traced out nearly a full period of their orbital motion which is governed by Kepler's laws. By assuming that the system has no angular momentum, and given the current separation, velocity of approach, and the age of the Universe, the timing argument yields estimates for the mass of the Local Group ( $> 3 \times 10^{12} M_{\odot}$ ), the semi-major axis of the orbit ( $< 580$  kpc), and the time of the next close passage ( $> 4$  Gyr) (see Sec. 10.2 of Binney & Tremaine 1987).

While the seminal results of Kahn & Woltjer (1959) were an early indication of the large mass-to-light ratio in the Local Group and therefore the presence of dark matter, they also began a nearly five decade long quest to understand the past, present, and future of our Local Group. In particular, a number of studies have extended the original timing argument by allowing for various angular momenta, by including more realistic or time-

<sup>\*</sup> tcx@cfa.harvard.edu

<sup>†</sup> loeb@cfa.harvard.edu

dependent mass distributions, or by adding the effects of mass at scales beyond that of the Local Group (see, e.g., Peebles et al. 1989; Fich & Tremaine 1991; Valtonen et al. 1993; Peebles 1994; Peebles et al. 2001; Sawa & Fujimoto 2005; Loeb et al. 2005).

One of the most intriguing developments stemming from the various studies of the Local Group is an estimate of the transverse velocity of Andromeda. By employing the action principle to the motions of galaxies within and near ( $< 20$  Mpc) the Local Group, Peebles et al. (2001) concluded that the transverse velocity of Andromeda is less than  $200 \text{ km s}^{-1}$ . Using the well measured transverse velocity of M33 and numerical simulations that tracked the potential tidal disruption during M33's past encounters with Andromeda, Loeb et al. (2005) found an even smaller estimate,  $\sim 100 \text{ km s}^{-1}$ , for the transverse velocity. While future astrometric observations using SIM<sup>1</sup> and GAIA<sup>2</sup> will be able to accurately measure the proper motion of Andromeda, the low values favored by these papers suggests that the Local Group is indeed a gravitationally bound system.

Provided that the Local Group is gravitationally bound, and that the Milky Way and Andromeda are heading towards each other, one must admit the possibility that they will eventually interact and merge. This outcome appears inevitable given the massive halos of dark matter that likely surround the Milky Way and Andromeda. Numerical experiments have robustly concluded that dark matter halos can exert significant dynamical friction, and are sponges that soak up energy and angular momentum leading to a rapid merger (Barnes 1988).

Even though the eventual merger between the Milky Way and Andromeda is common lore in Astronomy, the merger process has not been addressed by a comprehensive numerical study. The one exception is a paper by Dubinski et al. (1996) that presented a viable model for the Local Group and numerically simulated the eventual merger between the Milky Way and Andromeda. However, Dubinski et al. (1996) utilized this Local Group model and its numerical evolution to study the production of tidal tails during such an encounter and the possibility to use the structure of this tidal material to probe the dark matter potential. While the study by Dubinski et al. (1996) provided the first enticing picture of the future encounter between the Milky Way and Andromeda, (for a more recent and higher resolution version of this simulation, see Dubinski 2006), it was neither designed to detail the merger dynamics including intergalactic material, nor outline the possible outcomes for the dynamics of our Sun, nor quantify properties of the merger remnant. In addition, the last decade has produced a number of improved models for the structure of the Milky Way and Andromeda as well as the properties of the intra-group medium.

In this paper we quantitatively predict when the interaction and merger of the Milky Way and Andromeda will likely occur and forecast the probable dynamics of the Sun during this event. We achieve this goal by constructing a model for the Local Group in §2 that satisfies all observational constraints. We then evolve this model using a self-

consistent N-body/hydrodynamic simulation, as described in §3. The generic properties of the merger, including the merger timescale, the possible evolution of our Solar System, and properties of the merger remnant, are outlined in §4. Finally, we conclude in §5.

## 2 A MODEL OF THE LOCAL GROUP

The distribution of mass within our Local Group of galaxies has been a long-standing question in astrophysics. It is clear that much of the matter is associated with the two largest galaxies in the Local Group: the Milky Way and Andromeda. Moreover, these two spiral galaxies are likely to be embedded in an ambient medium of dark matter and gas.

There are a number of different models for both the Milky Way and Andromeda galaxies (see, e.g., Klypin et al. 2002; Widrow & Dubinski 2005; Seigar et al. 2006, and reference therein). These studies generally enlist a myriad of observational data to infer the distribution of baryons, while the dark matter, which dominates the gravitational potential, is set to match distributions extracted from cosmological N-body simulations (e.g., Navarro et al. 1996). Together, these models specify the total mass distribution out to the virial radius ( $\sim 200 - 300$  kpc).

In our model of the Local Group we start by adopting the models for the Milky Way and Andromeda favored by Klypin et al. (2002). Within these models, the baryons are contained entirely within the rotationally supported exponential disk and central bulge. These components are then surrounded by a massive dark-matter halo, which has nearly 20 times the mass as the baryons, as specified by the mass fractions,  $m_b$  and  $m_d$ , defined as the bulge and disk mass, respectively, divided by the total mass. The exponential disk, of radial disk scale radius  $R_d$ , also contains a set fraction  $f$  of its mass in collisional gas that can cool and form stars. Both the bulge and dark halo components are assumed to follow the Hernquist (1990) profile. The bulge scale radius  $a$  is fixed to be 20% of the radial disk scale radius  $R_d$ . The dark-matter profile is defined by its concentration  $c$ , spin parameter  $\lambda$ , and total virial mass  $M_{200}$  and virial circular velocity  $V_{200}$  (at the radius  $r_{200}$  where the average interior density is 200 times the critical cosmic density today,  $\rho_{\text{crit}} = 10^{-29} \text{ g cm}^{-3}$ ), which are all listed in Table 1. The numerical construction of these models employs methods commonly used to construct equilibrium disk galaxies (see, e.g., Hernquist 1993a; Springel & White 1999; Springel 2000; Cox et al. 2006; Springel et al. 2005).

Given the adopted parameters of the two largest galaxies in the Local Group, we must now define their orbital parameters and any ambient medium in which the system will be embedded. There are a few empirical constraints that must be considered. First, at the current epoch, the separation between the Milky Way and Andromeda is 780 kpc (McConnachie et al. 2005; Ribas et al. 2005). Second, the Milky Way and Andromeda are approaching each other at a radial speed of  $120 \text{ km s}^{-1}$ , assuming a local circular speed of  $220 \text{ km s}^{-1}$  (see Sec. 10.2 of Binney & Tremaine 1987). These observational facts tightly constrain any dynamical model of the Local Group since their fractional error bars are estimated to be less than  $\sim 5\%$ .

Less well constrained is the current estimate for the

<sup>1</sup> <http://planetquest.jpl.nasa.gov/SIM/>

<sup>2</sup> <http://www.sci.esa.int/gaia/>

**Table 1.** Properties of the Milky Way (MW) and Andromeda (M31) models used in the work (see text for definitions).

Property	MW	Andromeda
$V_{200}$ (km s <sup>-1</sup> )	145	170
$M_{200}$ (10 <sup>12</sup> M <sub>⊙</sub> )	1.0	1.6
$c$	12	12
$\lambda$	0.031	0.036
$m_d$	0.041	0.044
$R_d$	2.2	3.6
$f$	0.3	0.3
$m_b$	0.008	0.012
$a$	0.4	0.7
$N_{dm}$	475,500	755,200
$N_{disk}$	14,350	24,640
$N_{gas}$	6,150	10,560
$N_{bulge}$	4,000	9,600

transverse velocity of Andromeda. As mentioned in §1, speeds of  $< 200$  km s<sup>-1</sup> are favored by recent models (Peebles et al. 2001; Loeb et al. 2005), but depend upon assumptions regarding the distribution of mass within the Local Group and its initial state. We will therefore gauge the success of our Local Group model by its ability to reproduce the above three observations, but it should be kept in mind that the first two observations have significantly less leeway than the third.

One plausible starting model for the Local Group is to follow the logic originally employed by the timing argument (Kahn & Woltjer 1959), i.e., that the mass of the Local Group is entirely contained within the Milky Way and Andromeda and their motion is a simple two body problem governed by Kepler’s equations. In practice, however, most of the recent implementations of the timing argument (see, e.g., Binney & Tremaine 1987; Fich & Tremaine 1991) generally yield masses for the Local Group ( $> 3 \times 10^{12}$  M<sub>⊙</sub>) that exceed the total masses in our Milky Way and Andromeda models ( $2.6 \times 10^{12}$  M<sub>⊙</sub>). This discrepancy suggests that the Milky Way and Andromeda do not contain the entire quantity of mass in the Local Group and are instead the most massive concentrations of mass within a larger all-encompassing medium. This point of view is very natural in a cosmological context where galaxies are not isolated islands, but rather mountain peaks within a vast continent of land.

For these reasons our Local Group model supplements the Milky Way and Andromeda galaxy models with a diffuse and extended intragroup medium, as schematically depicted in Figure 1. Put within a cosmological framework this initial configuration may represent a point in time when the entire Local Group has decoupled from the general Hubble flow and is in the process of collapsing to become a virialized structure.

For simplicity, we assume that initially the Local Group medium is a constant density cube of 1.5 Mpc on a side composed of both dark matter and gas. The total diffuse mass within this cube is set equal to the total mass of the two galaxy halos today,  $2.6 \times 10^{12}$  M<sub>⊙</sub>, yielding a net mass interior to the MW/M31 orbit that is consistent with the timing argument. Our choice is motivated by other cosmological simulations (Gao et al. 2004) which indicate that a

substantial fraction of the dark matter is likely to be diffuse, residing in between virialized halos (within the unvirialized Local Group) at the initial time of our simulation 5Gyr ago.<sup>3</sup> We also postulate that the Local Group volume contains close to the cosmic mean value of baryons, namely 16% (Spergel et al. 2003). Since the Milky Way and Andromeda galaxy models only include baryons in the galactic disk and bulge components, they are far short of this value. We therefore set the Local Group medium to be 20% primordial gas, by mass, so that the entire region approaches the cosmic mean value. The gaseous component, like the dark matter, is initialized to have a constant density, and its temperature is fixed to be  $3 \times 10^5$  K, consistent with estimates for the warm-hot intergalactic medium at comparable overdensities from cosmological simulations (see, e.g., Fig. 6 in Davé et al. 2001). We note that the gas temperature is far below the virialized temperature of the Local Group, however this assumption is consistent with the post-turn around, and pre-virialized initial conditions that we adopt. Since most of the gas will be shocked and heated during the collapse and relaxation of the Local Group, the basic results of our simulation do not depend on this initial gas temperature.

Since the total mass of the diffuse medium is equivalent to the two galaxies, the two components are represented with an equivalent number of particles; 1.3 million (1.04 million dark matter, and 260,000 gas). With these assumptions, the overdensity of our initial Local Group model is  $\delta_{LG} = \rho_{LG}/\rho_{crit} \approx 10$ .

Unfortunately, once the Local Group contains this extended mass distribution the relative motion of the Milky Way and Andromeda no longer becomes a trivial application of Kepler’s laws. The diffuse mass will steadily extract orbital energy and angular momentum owing to dynamical friction, and the deep potential wells of the galaxies will slowly accrete diffuse matter. Both of these effects act to gradually extract energy from the binary system, hardening its orbit, and accelerating the merging process.

Owing to the complicated nature of the orbit, and its deviation from simple two-body motion, we are left with a fair degree of ambiguity regarding the initial state of our Local Group model. Because the configuration envisaged by Figure 1 resembles the cosmological collapse of an overdense region of the Universe, a natural starting point is when this fluctuation decoupled from the general cosmological expansion, turned around, and began to collapse under its own self gravity. Like the original timing argument, we then presume that this scenario also occurred for the Milky Way and Andromeda as well, i.e., we initialize their radial velocity to be zero as if they have just turned around and are now about to begin their gravitational collapse.

While some insight about the value of the turn around

<sup>3</sup> The initial scale of the Local group in our simulation is an order of magnitude larger than the virial radius  $r_{200}$  of the Milky Way or Andromeda galaxies. If one were to extend the Navarro et al. (1997) density profile of the envelope around each galaxy (with an asymptotic radial dependence of  $r^{-3}$ ) out to our initial Local Group scale, then one would roughly double the mass found within the virial radius of each halo. The added mass in that case would be similar to the amount we indeed assume for the intragroup medium.

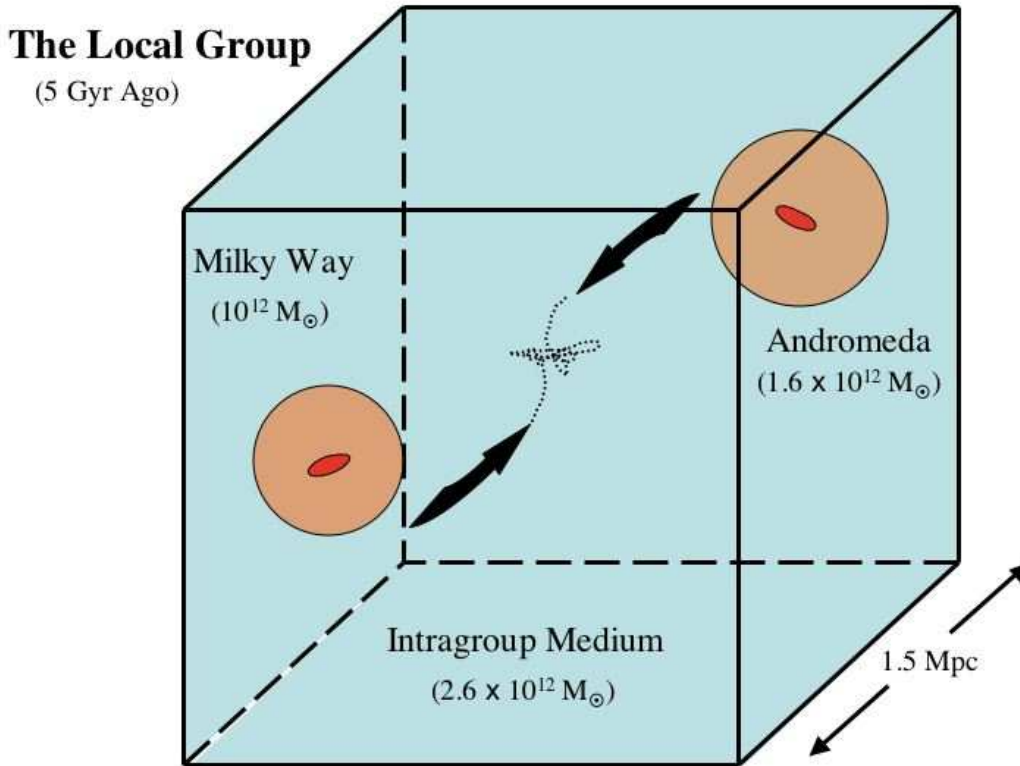


**Figure 1.** Sketch of the initial configuration of our Local Group model, which consists of the Milky Way and Andromeda embedded in a diffuse, constant-density intragroup medium of equivalent mass. See the text in §2 and Table 1 for more details.

radius can be gained from an application of the timing argument, in practice we find that the position and velocity of the Milky Way and Andromeda quickly deviated from simple two-body motion owing to the diffuse intragroup medium. In general, the velocities quickly grew larger than the original orbit specified and the direction became highly radial. We therefore adopted a trial and error approach where we build an initial model, run it until the Milky Way and Andromeda are separated by 780 kpc (as this is their current separation), and inspect the relative velocity between the two galaxies to assess the validity of the model.

Employing this procedure results in a best fitting model for the Local Group that begins with an initial Milky Way and Andromeda separation of 1.3 Mpc, and initializes the two objects on an eccentric orbit  $\epsilon = 0.494$ , with a distance at perigalacticon of 450 kpc and apogalacticon of 1.3 Mpc. With this orbit the initial angular velocity is  $65 \text{ km s}^{-1}$ , which could likely originate from tidal torques (Gott & Thuan 1978; Raychaudhury & Lynden-Bell 1989).

### 3 NUMERICAL METHODS

To simulate the evolution of our Local Group and in particular the interaction between the Milky Way and Andromeda we use the publically available N-body/hydrodynamic code GADGET2 (Springel 2005). This version of the code employs the “conservative-entropy” formulation of Smoothed Particle Hydrodynamics (SPH, Springel & Hernquist 2002) that conserves both energy and entropy (unlike earlier ver-

sions of SPH; see e.g., Hernquist 1993b), while improving shock-capturing. We assume that the gas is of primordial composition, and include the effects of radiative cooling.

Star formation and its associated feedback are both included in a manner very similar to that described in Cox et al. (2006). As is commonly assumed, stars are stochastically formed at a rate determined by the SPH gas density (see, e.g. Katz 1992; Springel & Hernquist 2003; Springel et al. 2005; Cox et al. 2006) with an efficiency set to match the observed correlation between star formation and gas density (Kennicutt 1998).

Feedback from stellar winds and supernovae is treated in a very simplistic manner, namely the SPH particles that have sufficient density to form stars are fixed to have an effective temperature of  $10^5 \text{ K}$ . This methodology is similar in principle to most of the currently favored models for feedback (see, e.g., Springel 2000; Springel & Hernquist 2003; Stinson et al. 2006; Cox et al. 2006), and is easy to implement. Since the focus of this work is the large-scale evolution of the Local Group and the generic dynamics of the collision between the Milky Way and Andromeda, the detailed treatment of the inter-stellar medium does not influence our primary conclusions.

### 4 THE COLLISION BETWEEN THE MILKY WAY AND ANDROMEDA

In Figures 2 through 6 we present the basic properties of the dynamical evolution of our Local Group, from 5 Gyr

in the past and until 10 Gyr into the future, beyond the merger time between the Milky Way and Andromeda. Most of the features present in these figures are generic to binary galaxy interactions, and have been described in great detail by prior studies (see, e.g., Toomre & Toomre 1972; Barnes & Hernquist 1991, 1992; Mihos & Hernquist 1996; Cox et al. 2006). However, we will review some of the details that are particularly relevant to the Local Group, and subsequently highlight the unique dynamics of the Sun as a test particle in this galaxy interaction process. The future evolution of structures beyond the local group was simulated elsewhere (Nagamine & Loeb 2003, 2004; Busha et al. 2003, 2005).

To begin, Figures 2 and 3 present the entire evolution of the Local Group from the point of view of a distant observer. These images begin at the start of our simulation, when the Milky Way and Andromeda are separated by 1.3 Mpc, and include the present state of the Local Group (labeled “Today”) and the eventual merger of the Milky Way and Andromeda. As a guide to the eye, each panel includes the trajectory of both the Milky Way and Andromeda.

Shown in Figure 2 is the evolution of the stellar component, which in our simulation only has contributions from the Milky Way and Andromeda as we ignore any structure smaller than the two largest galaxies in the Local Group.

Figure 3 presents the projected gas distribution during the interaction, with panels shown at the same times as in Figure 2. Here the color-scale has been stretched to emphasize the abundant quantity of low-density gas that is spread throughout the local group. The initial condition of our Local Group model assumes a uniform distribution of warm gas, however the gas quickly responds to the non-uniform potential. In particular gas is accreted and shocked to form a hydrostatic halo of warm gas around the Milky Way and Andromeda galaxies. The gas distribution is also clearly affected by the interaction itself, as shocks develop once the galaxy halos begin to interpenetrate at close separation.

While a detailed analysis of the diffuse gaseous intragroup medium is beyond the primary focus of our work, the basic properties of this component appear to be consistent with observations. In particular, our model predicts that, at the present state, the intragroup medium is predominantly warm  $10^5 - 10^6$  K, has a fairly low density,  $10^{-4} - 10^{-6}$  cm $^{-3}$ , and fills the entire volume that we simulate. We note this medium is also expected to extend to larger scales into what has been termed the “Warm-Hot Intergalactic Medium” (Cen & Ostriker 1999; Hellsten et al. 1998; Davé et al. 2001). While the presence of our intragroup medium is consistent with all current data (Osone et al. 2002). Owing to the difficulty in directly observing gas in this state, most evidence for its existence comes from indirect means. For example, *Chandra* and *FUSE* observations of  $z \sim 0$  Oxygen and Neon absorption along numerous sightlines suggests the presence of a local, volume-filling, diffuse, warm medium (Nicastro et al. 2002, 2003; Sembach et al. 2003; Savage et al. 2003), although detailed analysis of the ionization states suggest that this is a complex multi-phase medium that our simulation does not have the resolution to model.

While Figure 2 presented the dynamical evolution of the stellar mass on large scales, this vantage point makes it difficult to distinguish the tell-tale signs of a galaxy merger. We

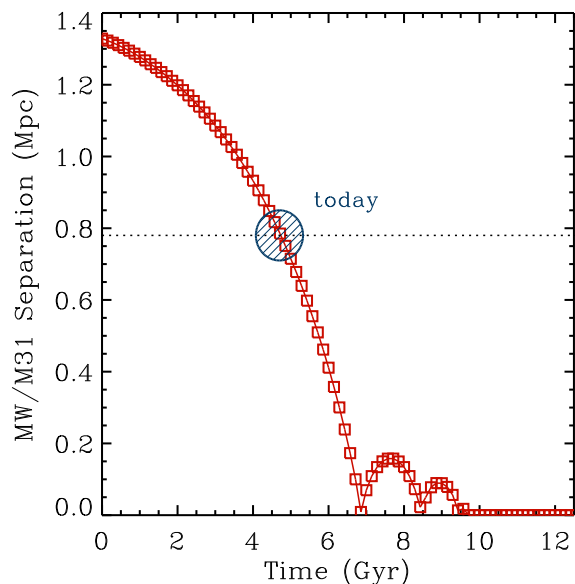


**Figure 5.** The separation between the centers of Andromeda and the Milky Way during the course of their merger. The current separation of  $\sim 780$  kpc is shown with a horizontal dashed line and occurs at  $T \approx 4.7$  Gyr.

therefore zoom into the central regions of the Local Group and specifically show the merger between the Milky Way and Andromeda in Figure 4. From this viewpoint the classic signatures of a galaxy interaction, such as tidal tails, plumes, and shells are clearly evident.

The physical separation between the Milky Way and Andromeda is presented in Figure 5. The current state of the Local Group occurs  $\sim 5$  Gyr after the start of our simulation. For the standard set of cosmological parameters (Tegmark 2006), this implies that we initiate the simulation at a redshift of  $z \approx 0.5$ , around the time when the Sun was born in the Milky Way disk<sup>4</sup>. Figure 5 also clearly shows the prediction that our models make for the future collision between the Milky Way and Andromeda. Their first close passage will occur less than 2 Gyr from the present, and the centers are fully coalesced in less than 5 Gyr. These time scales are comparable to the lifetime of our Sun (Sackmann et al. 1993) and admit the possibility that an observer in the Solar System will witness some (or all) of the galaxy collision. We will return to this possibility in §4.2.2.

Finally, we present the relative velocity between the Milky Way and Andromeda in Figure 6. As in Figure 5 we clearly delineate the present state of the Local Group with a hatched region whose size corresponds to the errors estimated with the velocity measurements. We note that the velocities presented are relative to each galaxy’s center of mass, and do not correct for any motion relative to that.

Now that the general features of our Local Group model have been outlined, we next explore the validity of our

<sup>4</sup> Note that extending the simulation to significantly earlier times is not adequate since stellar ages imply that the two galactic disks (and presumably their halos) have not been fully assembled at  $z \gtrsim 2$  (Wyse 2007).

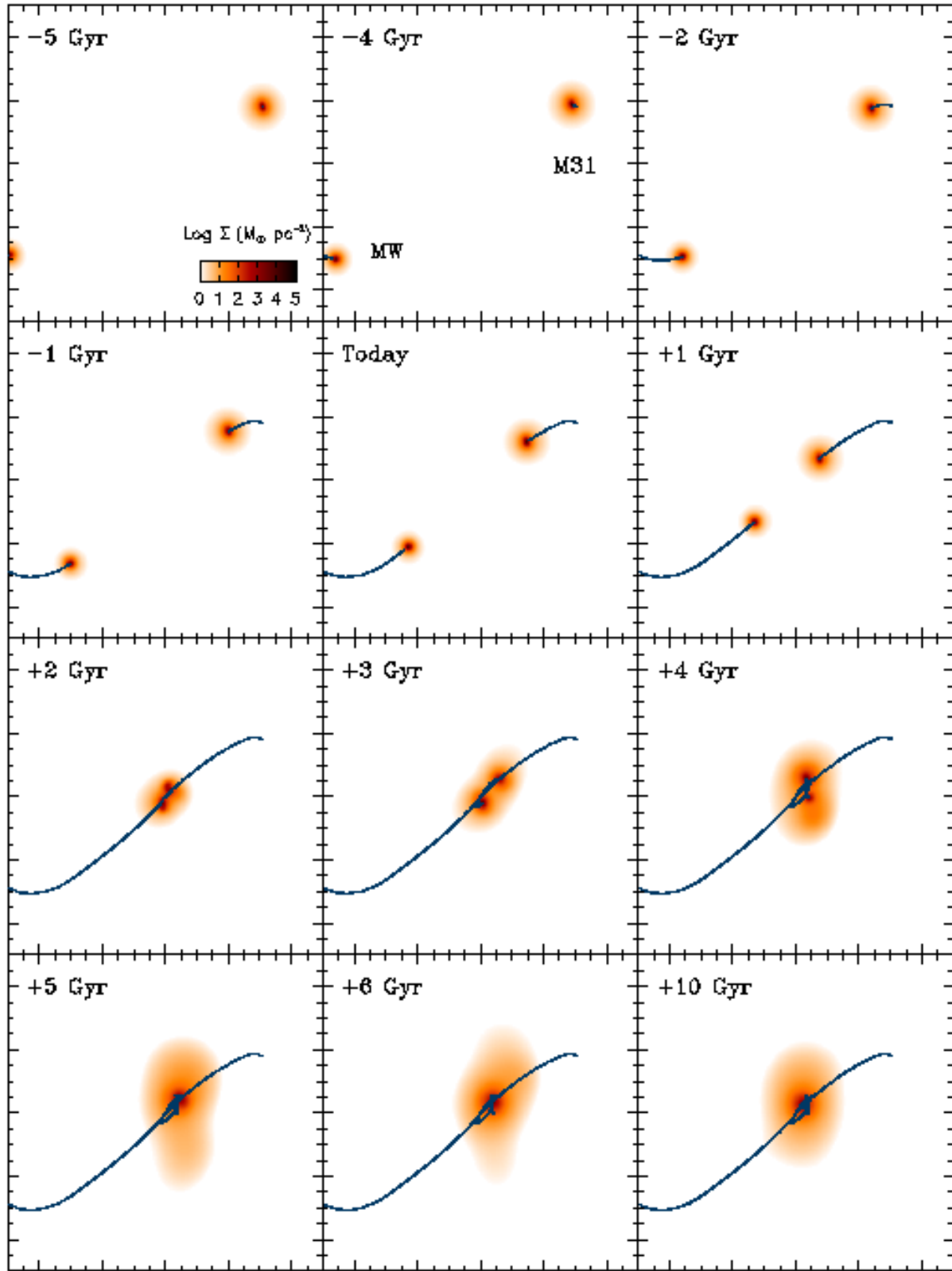


**Figure 2.** Time sequence of the projected stellar density, shown in red-scale, for the merger of the Milky Way (MW) and Andromeda (M31). Andromeda is the larger of the two galaxies and begins the simulation in the upper-right. The Milky Way begins on the edge of the image in the lower-left. Each panel is 1.5 Mpc square, and the simulation time, in Gyr relative to today, appear on the top-left label of each panel. The trajectories of the Milky Way and Andromeda are depicted by the blue solid lines.

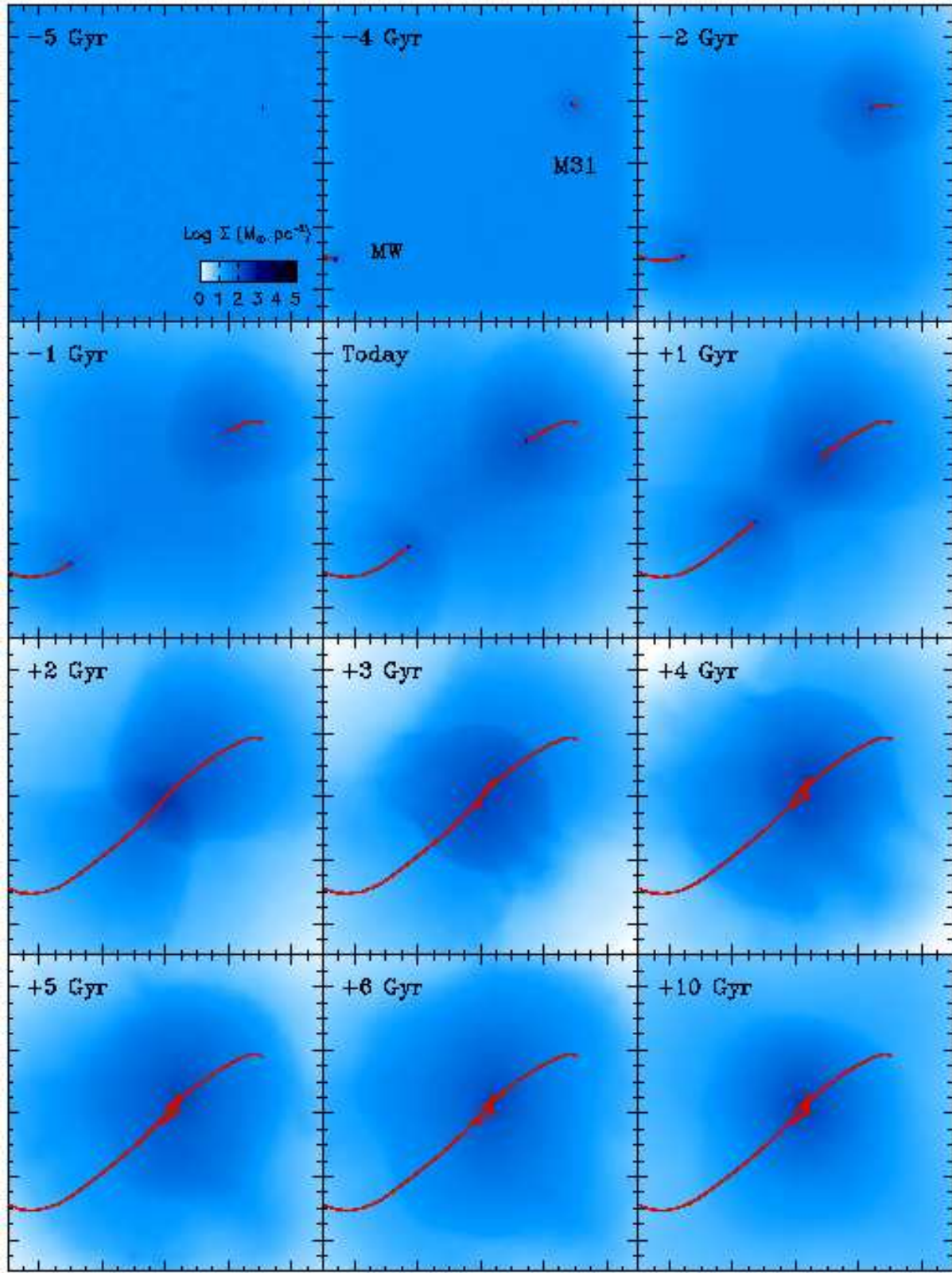
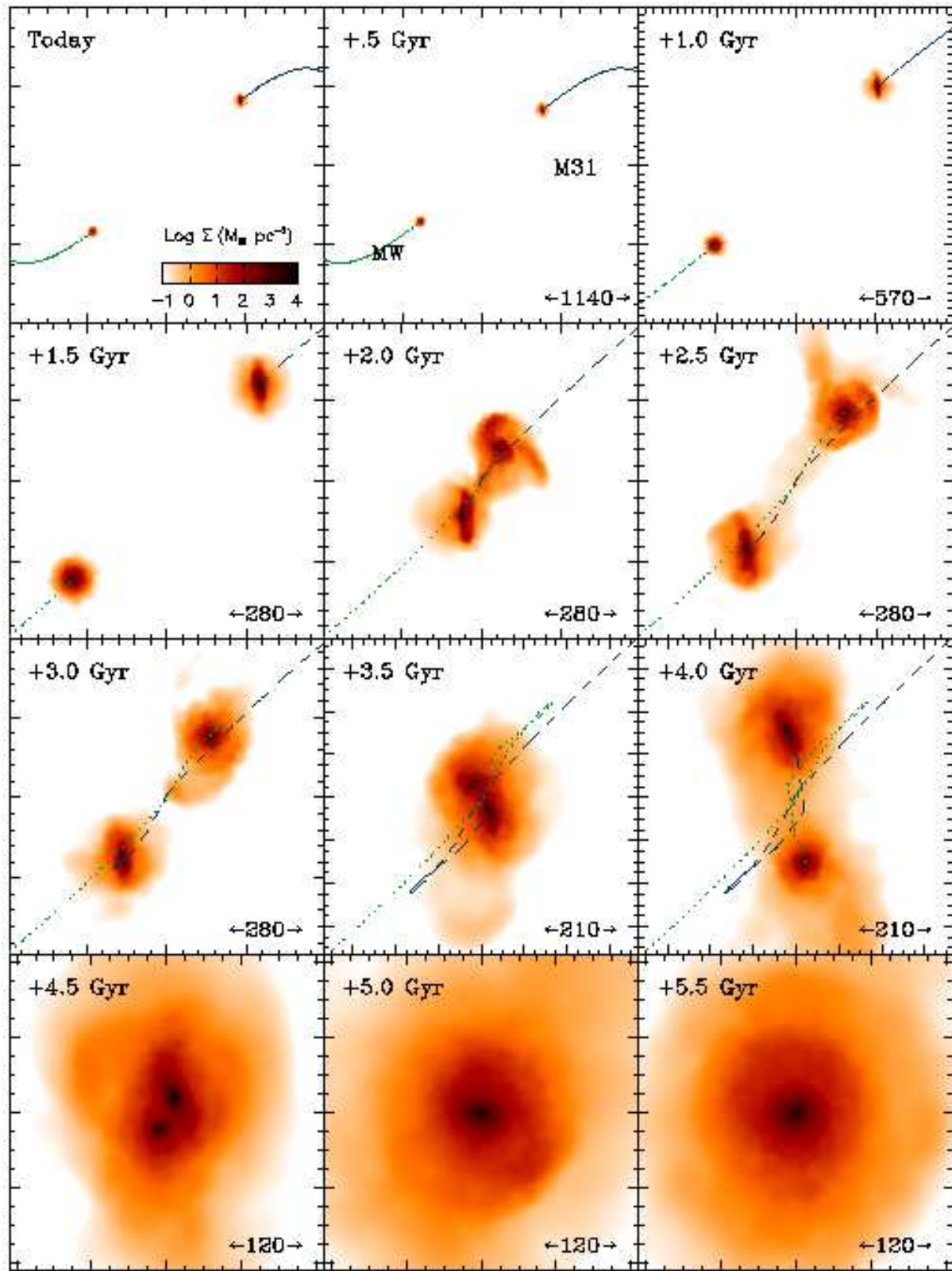
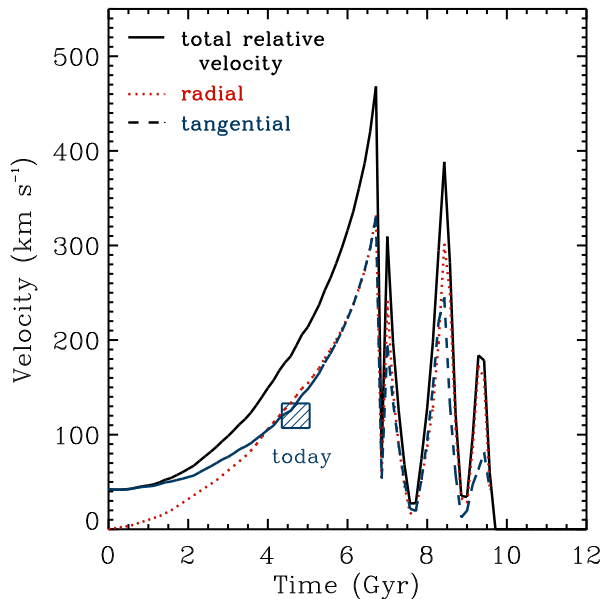


Figure 3. Same as Figure 2 only the projected gas density is shown.



**Figure 4.** Time sequence of the projected surface mass density of stars, during the final merger between Andromeda and the Milky Way. Panels have varying scales as specified by the label, in kpc, on the lower-right of each panel. The top-left panel is identical to the “Today” panel in Figure 2. The simulation time, with respect to today, is shown in the top-left of each panel.



**Figure 6.** The relative velocity between the centers of Andromeda and the Milky Way galaxies during the course of their merger. The present state of the Local Group occurs at  $T \approx 4.7$  Gyr.

model, the merger dynamics, the star formation during the interaction, and the properties of the merger remnant.

#### 4.1 The Current State of the Local Group

Although our model for the Local Group presents its past, current, and future evolution, the only way to test its validity is by comparing it to the empirical data on its present-day state. As we focus primarily on the evolution of the two largest galaxies in the Local Group, the Milky Way and Andromeda, it is only the relative separation and motion of these two galaxies that can be compared to data. As mentioned in both §1 and §4, the separation and line-of-sight velocity of the Milky Way and Andromeda are currently measured to be 780 kpc (McConnachie et al. 2005; Ribas et al. 2005, and references therein), and  $-120 \text{ km s}^{-1}$  (Binney & Tremaine 1987), respectively. The proper motion of Andromeda perpendicular to our line of sight is less well constrained, but current estimates suggest that it is  $< 200 \text{ km s}^{-1}$  (Peebles et al. 2001; Loeb et al. 2005).

Figures 5 and 6 present the direct comparisons between the observational constraints and our model, and clearly demonstrate that it is viable. In particular, at a time of 4.7 Gyr after the start of the simulation (close to the present cosmic time) the separation between the Milky Way and Andromeda is 780 kpc, while the relative radial velocity is  $135 \text{ km s}^{-1}$  and the tangential velocity is  $132 \text{ km s}^{-1}$ . While the tangential velocity is well within the limits currently favored, the line-of-sight velocity is slightly larger than (but within  $2.0 \sigma$  of) the observations. Even though a number of our model assumptions can be manipulated to reduce these values, e.g., the initial separation and eccentricity of the fiducial orbit, we note that our model is a good fit to the

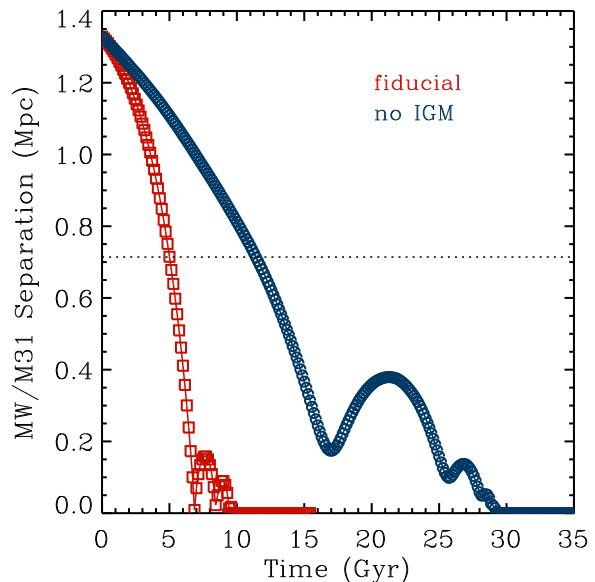


**Figure 7.** The separation between Andromeda and the Milky Way during the course of their merger. Our fiducial model in red is compared to a case with no intragroup medium (dark matter+gas) in blue. Dynamical friction on the diffuse medium shortens the MW/M31 coalescence time by a factor of a few. The present time is 5 Gyr after the start of the simulation.

velocity when the separation between the Milky Way and Andromeda is larger than 780 kpc. Given the observational uncertainties in these values we feel that there are likely to be a large number of models that can simultaneously fit all the data within its  $2\sigma$  error bars. We have explored a dozen additional models which yield comparable fits to the observational data. All these models displayed similar properties during the interaction in terms of their merger timescale, dynamics, and remnant properties.

#### 4.2 Merger Dynamics

##### 4.2.1 Timescale

One of the most intriguing characteristics of our Local Group model is the relatively quick timescale for the interaction and merger between the Milky Way and Andromeda. As stated in the previous section, their first close passage will occur in less than 2 Gyr, and the final coalescence will occur in less than 5 Gyr. While the following section will specifically address the possible dynamics of the Sun during the merger, we show here that the cause for the short merger timescale is the intragroup medium.

Our model for the Local Group assumes that the Milky Way and Andromeda are embedded in a diffuse medium of dark matter and gas. The medium itself (minus the evolved galaxies) is unvirialized and of low overdensity ( $\delta \sim 5$ ) corresponding to a region of the Universe that has decoupled from the Hubble flow and started its evolution toward a collapsed virialized state. This medium exerts dynamical friction on the Milky Way and Andromeda and speeds up the merger dynamics by soaking orbital energy and angular momentum. This is shown explicitly in Figure 7, which compares the

Milky Way – Andromeda separation in our fiducial model to an identical model without a diffuse medium. Without the intragroup medium, the merger timescale is nearly three times longer than with it.

The effect of the intragroup medium should scale similarly to the standard (Chandrasekhar) formula for dynamical friction (Binney & Tremaine 1987, Eq. 7-18), in which the deceleration of a massive object is proportional to the background matter density,  $dv/dt \propto \rho$ . Therefore, the rate at which angular momentum is extracted from the orbit depends on the assumed intragroup medium density, a quantity which is poorly constrained observationally. Once the dark matter halos begin to interpenetrate, i.e., when the Milky Way – Andromeda separation is  $\sim 100$  kpc, the merger completes relatively quickly because the dark matter halos dominate over the background density.

This last point is particularly relevant to simulations of binary galaxy mergers, which typically omit any background overdensity. While this omission does not significantly alter the dynamical friction estimates once the halos overlap and therefore dominate the background density, it may still change the distribution of orbits in high density environments where the galaxies traverse through significant overdensities prior to their interaction event. In this sense, the merger timescales extracted from binary merger simulations may be considered an upper limit that is most applicable to galaxies in the field.

#### 4.2.2 *The Fate of our Solar System*

An interesting consequence of the short timescale for the merger between the Milky Way and Andromeda is the possibility that a human (or decedent thereof) observer will witness the interaction and merger. At the heart of this issue is the comparison between the lifetime of the Sun and the interaction timescale.

Current evolutionary models (see, e.g., Sackmann et al. 1993) predict that the Sun will steadily increase its size and luminosity for the next 7 Gyr as it slowly consumes all available hydrogen and evolves towards a red giant phase. While this places a strong upper limit to the extent of life on Earth, it is likely that much smaller changes ( $< 50\%$ ) in the Sun’s luminosity will significantly alter the Earth’s atmosphere and thus its habitability within the next 1.1–3.5 Gyr (Kasting 1988). Korycansky et al. (2001) suggested that the onset of these effects could be delayed by increasing the orbital radius of the Earth through a sequence of interactions with bodies in the outer Solar System, and we can not rule out the possible colonization of habitable planets in nearby stars, especially long-lived M-dwarfs (Udry et al. 2007) whose lifetime may exceed  $10^{12}$  years (Adams et al. 2005). In short, it is conceivable that life may exist for as little as 1.1 Gyr into the future or, if interstellar travel is possible, much longer.

Regardless of the prospects for life in the future, we can predict what any potential observer at the solar Galactic circle might see by tracking candidate Suns in our simulation. In particular, we flag all stellar particles with a galactocentric radius of  $8 \pm 0.1$  kpc, corresponding to the observed value for the Sun (Eisenhauer et al. 2003), and subsequently follow the location of these particles forward in time. The results are presented in Figure 8. Given the uncertainties

in our model parameters, it is not possible to forecast reliably the actual phase of the Galactic orbit of the Sun at the time of closest approach to Andromeda. Therefore we regard all the stellar particles at the galactocentric of the sun as equally probable of being the Sun.

Figure 8 outlines the wide variety of potential locations for our candidate Suns during the future evolution of the Local Group. For example, the top–right panel in Figure 8 demonstrates the location of the candidate Suns after the first passage of Andromeda. At this point, the observer will most likely still be in the (now disturbed) disk of the Milky Way, but there exists a 12% chance that the Sun will be tidally ejected and take part in the tidal tail material that is  $> 20$  kpc away from the Milky Way center.

The probability that the candidate Sun will be located farther than 20 kpc from the Milky Way center steadily increases as the interaction progresses. At the second passage, the percentage of Suns that are farther than 20 kpc is 30%. This number increases to 48% after the second passage, and is 68% in the merger remnant. In fact, there is a 54% chance that the Sun will be at radii larger than 30 kpc in the merger remnant. However, we caution that this probability is derived at one point in time. Individual stars will generally spend much of their orbital time at large radii, even if their orbit is eccentric and they come much closer to the galactic center at other times.

One unexpected possibility for the location of the future Sun is demonstrated in the lower–middle panel of Figure 8, namely the Sun may actually become bound to Andromeda instead of the Milky Way before the two galaxies coalesce. Such a situation occurs when material becomes loosely bound after the first passage and is later captured by the gravitational potential of Andromeda during its second passage. While this outcome is unexpected and certainly exciting, only 2.7% of the candidate Suns became bound to Andromeda and so this outcome is relatively unlikely.

### 4.3 **Star Formation**

There is mounting evidence that galaxy interactions are the predominant mechanism for producing large bursts of star formation, such as in the ultra–luminous infrared galaxies (ULIRGs, Sanders & Mirabel 1996; Barnes & Hernquist 1992). During the interactions, gravitational torques extract angular momentum from the gas and funnel it to the center of the merger galaxy where it participates in a centrally–concentrated starburst. Because the future of the Local Group entails a major galaxy merger, it is natural to examine whether the merger of the Milky Way with Andromeda will become a ULIRG.

This question is addressed explicitly in Figure 9, which shows the star–formation rate during the entire evolution of the Local Group, including the merger between the Milky Way and Andromeda. Throughout the entire evolution of the Local Group, the star–formation rate steadily decreases with time, and hence we conclude that the merger Local Group will not become a ULIRG in the future. In fact, the final coalescence yields star formation that is barely enhanced above the that which would occur if the Milky Way and Andromeda has not participated in the merger at all.

The weak starburst event triggered by the merger between the Milky Way and Andromeda is a direct result of

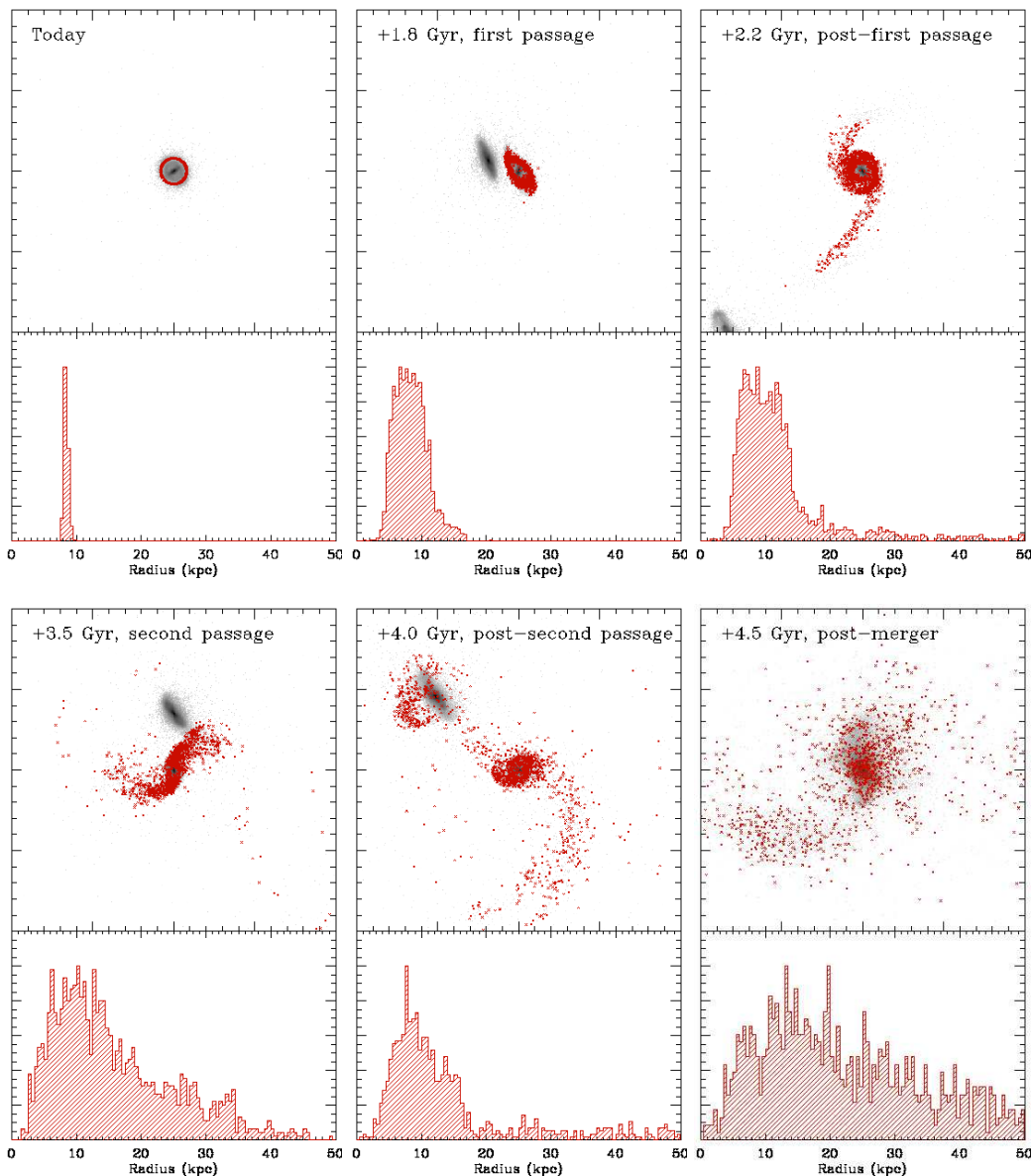


**Figure 8.** The possible location of the Sun during various stages of the merger between the Milky Way and Andromeda. The top panel shows all stellar particles in our simulation that have a present-day galactocentric radius of  $8 \pm 0.1$  kpc with a red cross and tracks their position into the future. The bottom panel presents a histogram of the radial distance from the center of the Milky Way.

their present low gas content. Moreover, a large fraction ( $> 75\%$ ) of this gas will be consumed by quiescent star formation by the time the merger actually occurs. In short, both disks will be extremely gas-poor during the final coalescence and there will be no fuel for the starburst.

While we have not explicitly tracked the black holes at the center of the Milky Way and Andromeda, it is interesting to speculate whether the merger will produce a luminous quasar, which many models argue is intricately linked to galaxy mergers and starbursts (Hopkins et al. 2006). Even though Figure 9 demonstrates that there is not enough gas to fuel a powerful starburst, this gas content is clearly sufficient to ignite a luminous quasar if  $\sim 1\%$  of it is accreted by the black hole. While the current work cannot address

this possibility in detail, our model provides a framework to study the formation of quasars in the future.

#### 4.4 The Merger Remnant

Galaxy mergers have become an area of intense study owing to their proposed role in shaping galaxy morphology. In particular, the “merger hypothesis” (Toomre 1977) posits that the interaction and merger of two spiral galaxies leaves behind a remnant that is morphologically and kinematically similar to an elliptical galaxy. Since the future evolution of the Local Group contains such an event, it is natural to examine whether the local group will eventually consist of a single elliptical galaxy, and if so, how do the properties

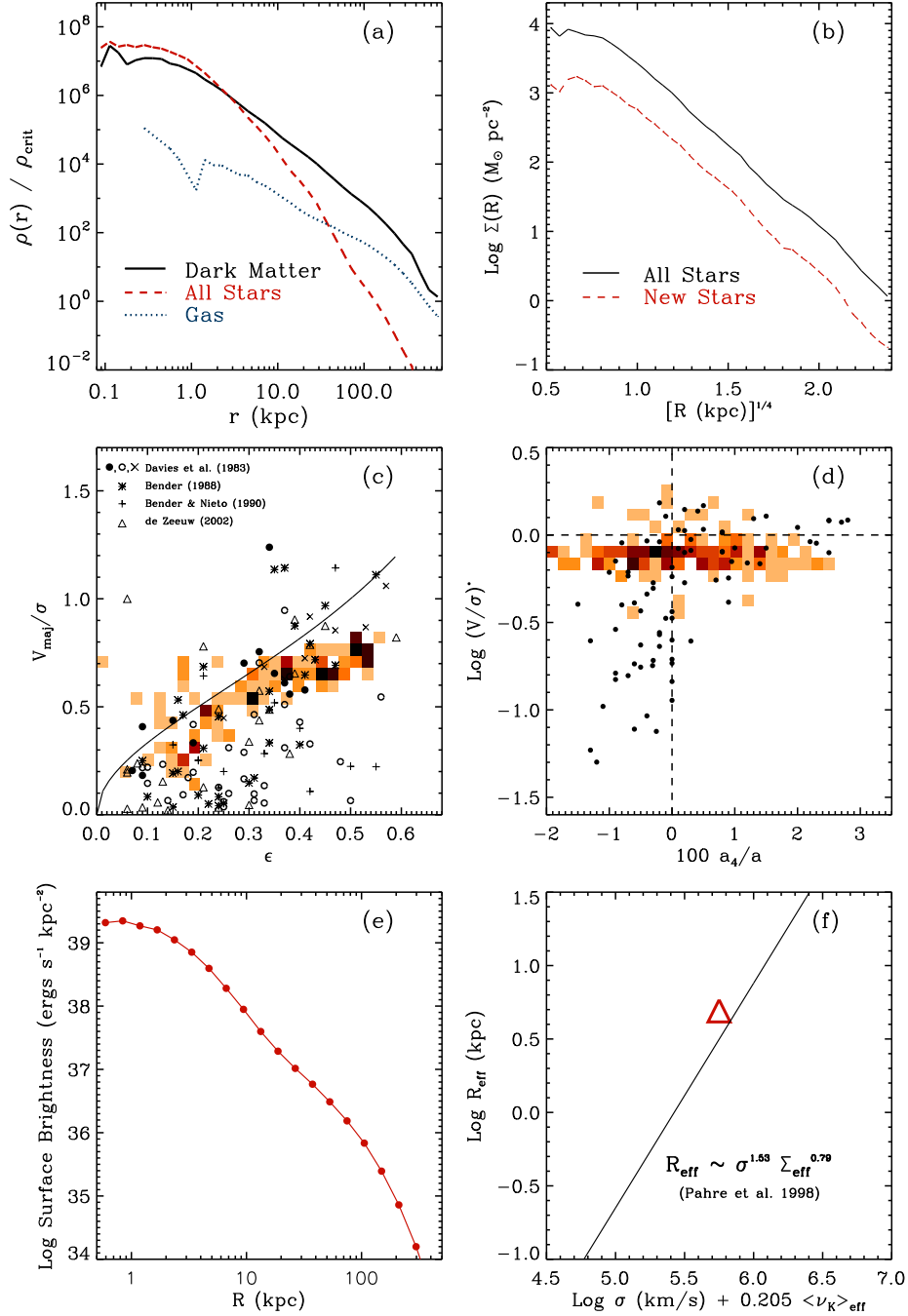


**Figure 10.** Properties of the Milky Way and Andromeda merger remnant, which we abbreviate as *Milkomeda*. Panel (a) shows the spherically averaged distribution of dark matter, stars, and gas. The mass density is expressed in units of the present-day critical density,  $\rho_{\text{crit}} = 10^{-29} \text{ g cm}^{-3}$ . Panel (b) shows the projected distribution of stellar mass, including the contribution from stars formed during the course of the simulation which are termed “New Stars,” plotted against  $R^{1/4}$ , where  $R$  is the projected radius. Panel (c) presents the kinematics of *Milkomeda*. For 195 projections, the ellipticity of the half-mass isophote  $\epsilon$ , the rotation velocity ( $V$ ) along the major axis  $V_{\text{maj}}$  and the central velocity dispersion  $\sigma$ , are plotted as a colored histogram, with darker shades representing a higher concentration of projected properties. The solid line represents what is expected from an oblate isotropic rotation and overplotted is data extracted from the literature. Panel (d) shows the velocity anisotropy, defined as the ratio  $V/\sigma$  normalized by the value expected for an oblate isotropic rotator, versus the isophotal shape parameter  $a_4/a$ , where positive values are disk-like isophotes and negative values are boxy. Overplotted in black are current data (Ralf Bender, private communication). Panel (e) shows the X-ray surface brightness profile, and panel (f) shows *Milkomeda* on the near-IR fundamental plane along with the relation observed by Pahre et al. (1998).

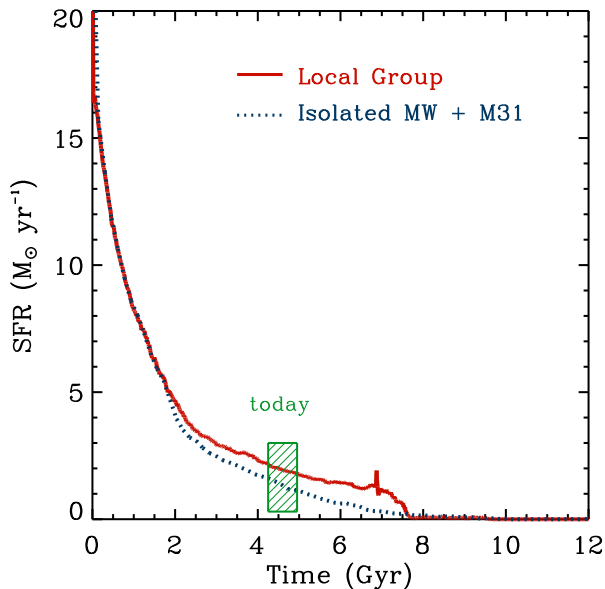


**Figure 9.** The cumulative star-formation rate during the merger of the Milky Way and Andromeda compared to the star formation for models of the Milky Way and Andromeda evolved in isolation.

of this galaxy differ from present-day ellipticals which were formed at earlier epochs.

Note that the morphology of the Milky Way and Andromeda merger remnant, which we abbreviate hereafter as *Milkomeda*, was presented in Figure 4. This figure confirms the notion that galaxy mergers leave behind remnants that are spheroidal in shape, contain stars with wide range of orbits and a large velocity dispersion, and possess very modest net rotation.

In Figure 10, we present a series of plots that further support the assertion that *Milkomeda* resembles an elliptical galaxy and also serve to better quantify its properties. In panel (a), we present the spherically averaged mass profile, decomposed by the three components; dark matter, stellar and gaseous mass. At radii greater than  $\sim 2\text{--}3$  kpc, the dark matter dominates the mass density, and at radii greater than  $\sim 20$  kpc, the profile is well-fit by the NFW (Navarro et al. 1996) or Hernquist (Hernquist 1990) profile.

The projected mass distribution shown in panel (b) of Figure 10 presents the first direct evidence that *Milkomeda* resembles an elliptical galaxy. Specifically, the stellar surface density is close to a pure  $R^{1/4}$  distribution, with the exception of the inner  $\sim 400$  pc, where the surface density flattens to a nearly constant density core.

We have also quantified the kinematics and isophotal shape of the *Milkomeda* galaxy following the methods of Cox et al. (2006). Panel (c) in Figure 10 presents the anisotropy diagram, a measure of the half-mass isophote ellipticity versus the maximum rotation along its major axis divided by the central velocity dispersion. The shaded region represents the distribution of values for *Milkomeda* if viewed from 195 directions that uniformly sample the unit sphere (with angles selected using HEALPIX, Górski et al. 2005). Also plotted in this figure is the relation expected from an oblate isotropic rotator as a solid line. Owing to the

high concentration of projections that closely track the solid line, this analysis demonstrates that *Milkomeda* is nearly an oblate isotropic rotator. In addition, the deviations from a perfect ellipse are also quantified and are presented in panel (d) in Figure 10. Depending on the viewing direction, *Milkomeda* may appear to be either disk-like or boxy, with a slightly larger fraction of views producing disk-like isophotes.

We have also analyzed the properties of the hot gas in and around *Milkomeda*. The evolution of this component was presented in Figure 3 and clearly demonstrates the formation of an extended gaseous halo, primarily accreted from the large reservoir of the intragroup medium. Although the gas temperature was originally  $3 \times 10^5$  K, it has been shock-heated to the virial temperature of  $\sim 3 \times 10^6$  K in *Milkomeda* and has a gradient to cooler temperatures at large radii. This hot gas leads to an X-ray surface brightness profile shown in panel (e) of Figure 10 and a total X-ray luminosity of  $\sim 10^{41}$  ergs  $s^{-1}$ , which is consistent with present-day elliptical galaxies of equivalent B-band luminosity ( $\sim 3 \times 10^{10} L_{\odot}$ ).

In general, *Milkomeda* resembles the remnants of gas-rich major mergers, which in-turn resemble the general population of low- and moderate-luminosity elliptical galaxies (Naab et al. 2006; Cox et al. 2006). However, there are some systematic differences that likely arise because of the much smaller gas content of the Milky Way and Andromeda when they merge. In particular, the inner regions of *Milkomeda* have a much lower stellar density than present-day ellipticals, which are often observed to have steep spikes of newly formed stars (Rothberg & Joseph 2004; Kormendy & Fischer 2007). These central excesses arise from high gas concentrations that fuel nuclear starbursts during the merger event (see, e.g., Mihos & Hernquist 1994; Springel 2000; Cox et al. 2006). This process does not occur during the formation of *Milkomeda* (see §4.3), for which the stars formed during the merger simulation have an identical profile to the entire stellar population (see panel (b) in Figure 10).

The diffuse nature of *Milkomeda* is also evident if it is projected onto the near-IR fundamental plane as shown in panel (f) of Figure 10, where it lies above the observed relation. The half-mass radius is 4.9 kpc, which is larger than the mean relation found in the Sloan Digital Sky Survey (Shen et al. 2003; Desroches et al. 2007) for galaxies of equivalent stellar mass ( $1.3 \times 10^{12} M_{\odot}$ ) or r-band absolute magnitude (-21.2). These comparisons give credence to the claim that present-day ellipticals can not have formed from the merger of present-day spirals (Naab & Ostriker 2007).

## 5 CONCLUSIONS

In this paper we have used an N-body/hydrodynamic simulation to track the evolution of the Local Group, focusing primarily upon the two most massive galaxies: the Milky Way and Andromeda. In contrast to most prior work, which typically employed models for the Local Group to infer its total mass or the proper motion of its constituents, we simulated the large-scale dynamics of all matter in the Local Group including dynamical friction on the intragroup medium, leading to the eventual merger of the Milky Way and Andromeda.

Owing to the diffuse intragroup medium that was as-

sumed to pervade the Local Group with a total mass comparable to that of the galaxies, we have found that the interaction and merger between the Milky Way and Andromeda will occur in less than 5 Gyr, a timescale comparable to the lifetime of the Sun (Sackmann et al. 1993). This Local Group model therefore admits the possibility that future astronomers in the Solar System will witness parts of, or the entire interaction and merger of the Milky Way and Andromeda.

With this in mind we have calculated the probable location of our Solar System during specific points of the future interaction and find several interesting outcomes. First, there is a 10% chance that the Sun will be ejected along with other tidal material into a long tidal tail following the first passage of Andromeda. Second, as a result of the disruptive effects of two close tidal passages there is a 50% chance that the Sun will inhabit extended tidal features after the second passage of Andromeda. Moreover, there is a 2.7% chance that the Sun will be more tightly bound to Andromeda at this point. In effect, Andromeda will capture the Sun and future astronomers in the solar system might see the Milky Way as an external galaxy in the night sky. Finally, the merger remnant contains a significantly heated stellar system compared to that of the Milky Way or Andromeda. Within the merger remnant there is a 67% chance that the Sun will reside at radii larger than 20 kpc (at least for the majority of its orbit).

While this paper highlights the possible outcomes of the future interaction between the Milky Way and Andromeda, we emphasize that our model is likely to be one of many plausible models within an ensemble of possibilities that span the uncertain value of the transverse velocity of Andromeda and the density of the intragroup medium. We have performed an additional dozen runs which yield similar agreement to the observational constraints as the model presented here and found little, if any, difference in our results. The results of these additional simulations suggest that our findings are robust to many of the modeling uncertainties. Nevertheless, a larger suite of models may provide better statistical confidence in the inferred merger timescale and the fate of our Sun and Local Group. In addition, employing higher resolution simulations with increased complexity, may shed light on the nature of the intragroup medium, the soft X-ray background (Osone et al. 2002), galactic substructure (Willman et al. 2005), the origin of the Magellanic Clouds and Stream (Besla et al. 2007), and the future evolution of globular clusters (Forbes et al. 2000).

Finally, we note that the simulated views from the distribution of locations for the candidate Suns in the merger remnant (see Fig. 8) represent the *only* views available for a future local astronomer. Extragalactic astronomy will come to an end within 100 billion years if the cosmological constant will not evolve with time. Owing to the accelerated expansion caused by a steady cosmological constant, all galaxies not bound to the Local Group will eventually recede away from the Local Group and exit our event horizon (Loeb 2002). At that point, the merger product of the Milky Way and Andromeda (with its bound satellites) will constitute the entire visible Universe (Nagamine & Loeb 2003).

## ACKNOWLEDGMENTS

The simulations were performed at the Center for Parallel Astrophysical Computing at the Institute for Theory and Computation at the Harvard-Smithsonian Center for Astrophysics. We acknowledge helpful discussions with G. Besla, S. Dutta, L. Hernquist, P. Hopkins, and B. Robertson. We thank Ralf Bender for kindly providing data used in Figure 10.

## REFERENCES

- Adams F. C., Bodenheimer P., Laughlin G., 2005, *Astronomische Nachrichten*, 326, 913  
 Barnes J. E., 1988, *ApJ*, 331, 699  
 Barnes J. E., Hernquist L., 1992, *ARA&A*, 30, 705  
 Barnes J. E., Hernquist L. E., 1991, *ApJL*, 370, L65  
 Besla G., Kallivayalil N., Hernquist L., Robertson B., Cox T. J., van der Marel R. P., Alcock C., 2007, *ArXiv Astrophysics e-prints*  
 Binney J., Tremaine S., 1987, *Galactic dynamics*. Princeton, NJ, Princeton University Press, 1987, 747 p.  
 Busha M. T., Adams F. C., Wechsler R. H., Evrard A. E., 2003, *ApJ*, 596, 713  
 Busha M. T., Evrard A. E., Adams F. C., Wechsler R. H., 2005, *MNRAS*, 363, L11  
 Cen R., Ostriker J. P., 1999, *ApJ*, 514, 1  
 Cox T. J., Dutta S., Di Matteo T., Hernquist L., Hopkins P. F., Robertson B., Springel V., 2006, *ApJ*, 650, 791  
 Cox T. J., Jonsson P., Primack J. R., Somerville R. S., 2006, *MNRAS*, 373, 1013  
 Davé R., Cen R., Ostriker J. P., Bryan G. L., Hernquist L., Katz N., Weinberg D. H., Norman M. L., O’Shea B., 2001, *ApJ*, 552, 473  
 Desroches L.-B., Quataert E., Ma C.-P., West A. A., 2007, *MNRAS*, 377, 402  
 Dubinski J., 2006, *S&T*, 112, 30  
 Dubinski J., Mihos J. C., Hernquist L., 1996, *ApJ*, 462, 576  
 Eisenhauer F., Schödel R., Genzel R., Ott T., Tecza M., Abuter R., Eckart A., Alexander T., 2003, *ApJL*, 597, L121  
 Fich M., Tremaine S., 1991, *ARA&A*, 29, 409  
 Forbes D. A., Masters K. L., Minniti D., Barmby P., 2000, *A&A*, 358, 471  
 Gao L., White S. D. M., Jenkins A., Stoehr F., Springel V., 2004, *MNRAS*, 355, 819  
 Górski K. M., Hivon E., Banday A. J., Wandelt B. D., Hansen F. K., Reinecke M., Bartelmann M., 2005, *ApJ*, 622, 759  
 Gott III J. R., Thuan T. X., 1978, *ApJ*, 223, 426  
 Hellsten U., Gnedin N. Y., Miralda-Escudé J., 1998, *ApJ*, 509, 56  
 Hernquist L., 1990, *ApJ*, 356, 359  
 Hernquist L., 1993a, *ApJS*, 86, 389  
 Hernquist L., 1993b, *ApJ*, 404, 717  
 Hopkins P. F., Hernquist L., Cox T. J., Di Matteo T., Robertson B., Springel V., 2006, *ApJS*, 163, 1  
 Kahn F. D., Woltjer L., 1959, *ApJ*, 130, 705  
 Kasting J. F., 1988, *Icarus*, 74, 472  
 Katz N., 1992, *ApJ*, 391, 502  
 Kennicutt R. C., 1998, *ApJ*, 498, 541

- Klypin A., Zhao H., Somerville R. S., 2002, *ApJ*, 573, 597  
 Kormendy J., Fischer D. B., 2007, *ApJ*, submitted, 000, 000  
 Korycansky D. G., Laughlin G., Adams F. C., 2001, *Ap&SS*, 275, 349  
 Loeb A., 2002, *PhRvD*, 65, 047301  
 Loeb A., Reid M. J., Brunthaler A., Falcke H., 2005, *ApJ*, 633, 894  
 McConnachie A. W., Irwin M. J., Ferguson A. M. N., Ibata R. A., Lewis G. F., Tanvir N., 2005, *MNRAS*, 356, 979  
 Mihos J. C., Hernquist L., 1994, *ApJL*, 437, L47  
 Mihos J. C., Hernquist L., 1996, *ApJ*, 464, 641  
 Naab T., Jesseit R., Burkert A., 2006, *MNRAS*, 372, 839  
 Naab T., Ostriker J. P., 2007, *ArXiv Astrophysics e-prints*  
 Nagamine K., Loeb A., 2003, *New Astronomy*, 8, 439  
 Nagamine K., Loeb A., 2004, *New Astronomy*, 9, 573  
 Navarro J. F., Frenk C. S., White S. D. M., 1996, *ApJ*, 462, 563  
 Navarro J. F., Frenk C. S., White S. D. M., 1997, *ApJ*, 490, 493  
 Nicastrro F., Zezas A., Drake J., Elvis M., Fiore F., Fruscione A., Marengo M., Mathur S., Bianchi S., 2002, *ApJ*, 573, 157  
 Nicastrro F., Zezas A., Elvis M., Mathur S., Fiore F., Cecchi-Pestellini C., Burke D., Drake J., Casella P., 2003, *Nature*, 421, 719  
 Osone S., Makishima K., Matsuzaki K., Ishisaki Y., Fukazawa Y., 2002, *PASJ*, 54, 387  
 Pahre M. A., de Carvalho R. R., Djorgovski S. G., 1998, *AJ*, 116, 1606  
 Peebles P. J. E., 1994, *ApJ*, 429, 43  
 Peebles P. J. E., Melott A. L., Holmes M. R., Jiang L. R., 1989, *ApJ*, 345, 108  
 Peebles P. J. E., Phelps S. D., Shaya E. J., Tully R. B., 2001, *ApJ*, 554, 104  
 Raychaudhury S., Lynden-Bell D., 1989, *MNRAS*, 240, 195  
 Ribas I., Jordi C., Vilardell F., Fitzpatrick E. L., Hilditch R. W., Guinan E. F., 2005, *ApJL*, 635, L37  
 Rothberg B., Joseph R. D., 2004, *AJ*, 128, 2098  
 Sackmann I.-J., Boothroyd A. I., Kraemer K. E., 1993, *ApJ*, 418, 457  
 Sanders D. B., Mirabel I. F., 1996, *ARA&A*, 34, 749  
 Savage B. D., Sembach K. R., Wakker B. P., Richter P., Meade M., Jenkins E. B., Shull J. M., Moos H. W., Sonneborn G., 2003, *ApJS*, 146, 125  
 Sawa T., Fujimoto M., 2005, *PASJ*, 57, 429  
 Seigar M. S., Barth A. J., Bullock J. S., 2006, *ApJ* submitted (astro-ph/0612228)  
 Sembach K. R., Wakker B. P., Savage B. D., Richter P., Meade M., Shull J. M., Jenkins E. B., Sonneborn G., Moos H. W., 2003, *ApJS*, 146, 165  
 Shen S., Mo H. J., White S. D. M., Blanton M. R., Kauffmann G., Voges W., Brinkmann J., Csabai I., 2003, *MNRAS*, 343, 978  
 Spergel D. N., Verde L., Peiris H. V., Komatsu E., Nolte M. R., Bennett C. L., Halpern M., Hinshaw G., Jarosik N., Kogut A., Limon M., Meyer S. S., Page L., Tucker G. S., Weiland J. L., Wollack E., Wright E. L., 2003, *ApJS*, 148, 175  
 Springel V., 2000, *MNRAS*, 312, 859  
 Springel V., 2005, *MNRAS*, 364, 1105  
 Springel V., Di Matteo T., Hernquist L., 2005, *MNRAS*, 361, 776  
 Springel V., Hernquist L., 2002, *MNRAS*, 333, 649  
 Springel V., Hernquist L., 2003, *MNRAS*, 339, 289  
 Springel V., White S. D. M., 1999, *MNRAS*, 307, 162  
 Stinson G., Seth A., Katz N., Wadsley J., Governato F., Quinn T., 2006, *MNRAS* submitted (astro-ph/0602350)  
 Tegmark M. e. a., 2006, *PhRvD*, 74, 123507  
 Toomre A., 1977, in *Evolution of Galaxies and Stellar Populations Mergers and Some Consequences*. p. p.401  
 Toomre A., Toomre J., 1972, *ApJ*, 178, 623  
 Udry S., Bonfils X., Delfosse X., Forveille T., Mayor M., Perrier C., Bouchy F., Lovis C., Pepe F., Queloz D., Bertaux J. ., 2007, *A&A* submitted (astro-ph/0704.3841), 704  
 Valtonen M. J., Byrd G. G., McCall M. L., Innanen K. A., 1993, *AJ*, 105, 886  
 Widrow L. M., Dubinski J., 2005, *ApJ*, 631, 838  
 Willman B., Dalcanton J. J., Martinez-Delgado D., West A. A., Blanton M. R., Hogg D. W., Barentine J. C., Brewington H. J., Harvanek M., Kleinman S. J., Krzesinski J., Long D., Neilsen Jr. E. H., Nitta A., Snedden S. A., 2005, *ApJL*, 626, L85  
 Wyse R. F. G., 2007, in *IAU Symposium Vol. 77 of IAU Symposium, Lessons from Surveys of The Galaxy*. pp 1036-1046